Theory and numerics of vibrational resonance in Duffing oscillators with time-delayed feedback

C. Jeevarathinam and S. Rajasekar[*]

School of Physics, Bharathidasan University, Tiruchirappalli 620 024, India

M. A. F. Sanjuán[†]

Nonlinear Dynamics, Chaos and Complex Systems Group, Departamento de Física, Universidad Rey Juan Carlos, Tulipán s/n,
28933 Móstoles, Madrid, Spain and Department of Mathematics, School of Science, Beijing Jiaotong University,
Beijing 100044, People's Republic of China

The influence of linear time-delayed feedback on vibrational resonance is investigated in underdamped and overdamped Duffing oscillators with double-well and single-well potentials driven by both low frequency and high frequency periodic forces. This task is performed through both theoretical approach and numerical simulation. Theoretically determined values of the amplitude of the high frequency force and the delay time at which resonance occurs are in very good agreement with the numerical simulation. A major consequence of time-delayed feedback is that it gives rise to a periodic or quasiperiodic pattern of vibrational resonance profile with respect to the time-delayed parameter. An appropriate time delay is shown to induce a resonance in an overdamped single-well system which is otherwise not possible. For a range of values of the time-delayed parameters, the response amplitude is found to be larger than in delay-time feedback-free systems.

I. INTRODUCTION

The response of a nonlinear system to a weak periodic signal can be enhanced by means of an appropriate noise [1], a high frequency periodic force [2], or a chaotic signal [3]. The enhancements of the response of a system due to the applied weak noise, a high frequency force, or a chaotic signal are termed as stochastic resonance, vibrational resonance, and chaotic resonance, respectively. Among them, much attention has been given to stochastic resonance and a lot of progress has been made. However, the analysis of vibrational resonance (VR) has also received considerable interest in recent years due to its importance in a wide variety of contexts in physics, engineering, and biology.

In a typical VR, when the amplitude g or the frequency Ω of a high frequency periodic force is varied, the amplitude of the response at the low frequency of the input signal reaches a maximum value at one or more critical values of g or Ω and then decays. Its occurrence has been analyzed by theoretical, numerical, and experimental procedures in certain nonlinear dynamical systems. For example, VR was studied both theoretically and numerically in multiwell systems [2,4–8] and in a single-well system [9]. An experimental demonstration of it in a bistable vertical-cavity surface-emitting laser [10–12], analog simulation of the overdamped Duffing oscillator [13], and the effect of an additive Gaussian white noise [13,14] were also reported. VR has also been found in excitable systems [15–17] and in small-world networks [18].

Numerical evidence for multiple VR induced by time-delayed feedback in overdamped uncoupled and coupled bistable systems [19,20] has been reported very recently. When the state of a system at time t depends on its state at a shifted earlier time, say $t − α$, then a time-delayed

feedback term is introduced in the equation of motion of the system. The feedback term can be linear or nonlinear. Time-delayed phenomena are ubiquitous in many nonlinear systems due to a finite switching speed of amplifiers, finite signal propagation time in biological networks, finite reaction times, memory effects, etc. [21–23]. In a variety of physical, engineering, biological, and chemical systems the presence of time-delayed feedback or time-delayed couplings is inevitable. Examples include propagation delays in networks [24], laser arrays [25–27], electronic circuits [28], and neural systems [29–31]. Time-delayed nonlinear systems are found to show interesting dynamical phenomena such as novel bifurcations [32,33], amplitude death [34], strange nonchaotic attractors [35], hyperchaos [36], stochastic dynamics [37–39], excitation regeneration [40], reentrance phenomena [41,42], and patterns [43]. However, the effect of time delay on VR has not been studied systematically. Thus, it is important to develop a theoretical approach to investigate and explore the role of time-delayed parameters on the mechanism of VR in time-delayed systems and also obtain an analytical expression for the values of the control parameters at which VR occurs.

Motivated by the above ideas, we present here a theoretical approach to investigate VR in underdamped and overdamped nonlinear systems with a delay feedback and driven by a bi-harmonic force. We apply it to the time-delayed underdamped Duffing oscillator

$$\ddot{x} + d\dot{x} + \omega_0^2 x + \beta x^3 + \gamma x(t - \alpha)$$
$$= f \cos \omega t + g \cos \Omega t \qquad (1)$$

and time-delayed overdamped Duffing oscillator

$$\dot{x} + \omega_0^2 x + \beta x^3 + \gamma x(t - \alpha) = f \cos \omega t + g \cos \Omega t, \quad (2)$$

where $\Omega \gg \omega$ and $\alpha > 0$ is the time-delayed parameter. In the absence of a damping term, external periodic forces, and feedback term, the potential of the Duffing oscillator is $V(x) = \frac{1}{2}\omega_0^2 x^2 + \frac{1}{4}\beta x^4$. $V(x)$ becomes a double well for $\omega_0^2 < 0$,

[*]rajasekar@cnld.bdu.ac.in
[†]miguel.sanjuan@urjc.es
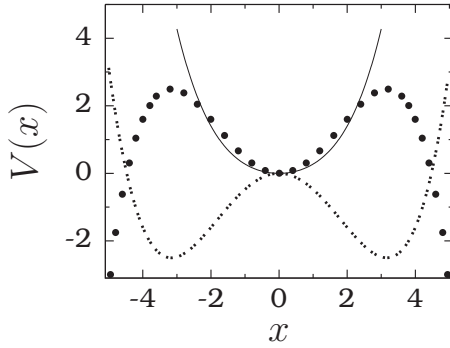
FIG. 1. Single-well (represented by a continuous line, $\omega_0^2 = 0.5$, $\beta = 0.1$), double-well (represented by a dashed line, $\omega_0^2 = -1$, $\beta = 0.1$), and single-well with double-hump (represented by solid circles, $\omega_0^2 = 1$, $\beta = -0.1$) forms of the potential $V(x) = \frac{1}{2}\omega_0^2 x^2 + \frac{1}{4}\beta x^4$.

$\beta > 0$, and a single well for $\omega_0^2, \beta > 0$, respectively. Moreover, for $\omega_0^2 > 0$, $\beta < 0$ the potential has a single well with double-hump form. These three forms of the potential are depicted in Fig. 1. For $\omega_0^2, \beta < 0$ the potential has an inverted single-well form. We consider both single-well and double-well cases of the underdamped and overdamped systems (1) and (2). Our main concern is to explore the interplay between the time delay and the high frequency force. For $\Omega \gg \omega$ and for $f \ll 1$, due to the different time scales of the forces $f \cos \omega t$ and $g \cos \Omega t$, it is reasonable to assume that the solutions of systems (1) and (2) essentially consist of a slow motion $X(t)$ and a fast motion $\psi(t, \Omega t)$. Through a theoretical approach, we obtain an analytical expression for the variables X and ψ for both systems (1) and (2). The amplitude of the fast motion is periodic in α with period $2\pi/\Omega$, while that of the slow motion has terms which are periodic in α with periods $2\pi/\omega$ and $2\pi/\Omega$. The ratio of the amplitude A_L of slow motion and f is termed as the response amplitude Q. From the theoretical expression of Q, we are able to determine the values of g and α denoted as g_{VR} and α_{VR}, respectively, at which VR occurs, i.e., Q becomes a maximum. Theoretical predictions of Q, g_{VR}, and α_{VR} are in very good agreement with numerical simulations.

There are certain common and distinct influences of the time-delayed feedback parameters α and γ in the four systems under analysis. These four systems are (1) underdamped double-well Duffing oscillator, (2) underdamped single-well Duffing oscillator, (3) overdamped double-well Duffing oscillator, and (4) overdamped single-well Duffing oscillator. When the amplitude g of the high frequency periodic force is treated as a control parameter, we find the following key results. In the underdamped double-well system two resonances occur for $|\gamma| < \omega^2/(1 - \cos \omega\alpha)$, otherwise only a single resonance occurs. Double resonance is not possible in the underdamped single-well system, however, a single resonance occurs for $\omega^2 - \gamma \cos \omega\alpha > \omega_0^2$. In the overdamped double-well system with and without time-delayed feedback one resonance always occurs at the critical value of g, g_c at which the effective potential of the slow variable undergoes a transition from a bistable (double-well) to a monostable (single-well) potential. In the absence of time-delayed feedback, a resonance is not at all possible in the overdamped single-well system. Interestingly, the inclusion of an appropriate time-delayed

feedback induces a resonance. In all four systems $Q(\gamma, g_{VR}) > Q(\gamma = 0, g_{VR})$ for a wide range of values of γ and α. When α is varied, in all four systems, the response amplitude Q is periodic (with period $2\pi/\omega$) or quasiperiodic on α depending upon whether the ratio Ω/ω is rational or irrational. The response amplitude profile is modulated by the high frequency force, however, the modulation period is not strictly $2\pi/\Omega$. For a range of values of γ and g we notice $Q(\gamma, \alpha_{VR}) > Q(\gamma = 0)$.

The organization of the paper is as follows. In Sec. II we consider the underdamped double-well and single-well systems. First, we obtain an approximate analytical expression for the response amplitude Q at the low frequency ω. For the double-well case we get the theoretical expressions for the amplitude g at which resonance occurs. Since it is difficult to find the analytical expression for α_{VR}, we calculate the numerical values of α_{VR} for a range of fixed values of γ and g from the theoretical expression of Q. Next we verify the theoretical predictions with the numerical simulation. We point out the mechanism of the resonance and compare the change in the slow motion $X(t)$ and the actual motion $x(t)$ when the control parameters g and α are varied. Then, we study the VR in the single-well system. Section III is devoted to the overdamped systems. For the double-well case, we show that a resonance always occurs at $g = g_c$ when g is varied. We determine α_{VR} for a range of fixed values of g and give examples for periodic and quasiperiodic patterns of VR. Then, we present the results for the single-well system. In Sec. IV we briefly discuss the limits of the applicability of the theoretical approach. Finally, in Sec. V, we summarize our findings.

II. UNDERDAMPED DUFFING OSCILLATOR

In this section we obtain a theoretical expression for the response amplitude Q in the presence of time-delayed feedback in the underdamped Duffing oscillator. Using this expression, we analyze the occurrence of VR in both double-well and single-well cases.

A. Theoretical expression for the response amplitude Q

We assume the solution of the system (1) for $\Omega \gg \omega$ as $x = X + \psi$, where $X(t)$ and $\psi(\tau = \Omega t)$ are a slow motion with period $2\pi/\omega$ in the time t and a fast motion with period 2π in the fast time τ, respectively. Further, we assume that the average value of ψ over the period 2π is $\psi_{av} = (1/2\pi) \int_0^{2\pi} \psi \, d\tau = 0$. The equations of motion of X and ψ are

$$\ddot{X} + d\dot{X} + (\omega_0^2 + 3\beta\psi_{av}^2)X + \beta(X^3 + \psi_{av}^3) + \gamma X(t - \alpha)$$
$$+ 3\beta X^2 \psi_{av} = f \cos \omega t, \tag{3}$$

$$\ddot{\psi} + d\dot{\psi} + \omega_0^2 \psi + 3\beta X^2(\psi - \psi_{av}) + 3\beta X(\psi^2 - \psi_{av}^2)$$
$$+ \beta(\psi^3 - \psi_{av}^3) + \gamma \psi(\tau - \Omega\alpha) = g \cos \Omega t, \tag{4}$$

where $\psi_{av}^n = (1/2\pi) \int_0^{2\pi} \psi^n \, d\tau$. Neglecting the nonlinear terms in Eq. (4), the solution of the linear version in the limit $t \to \infty$ is given by

$$\psi = \frac{g}{\mu} \cos(\tau + \phi), \tag{5a}$$

where
$$\mu^2 = \left(\omega_0^2 - \Omega^2 + \gamma\,\cos\,\Omega\alpha\right)^2 + (-d\Omega + \gamma\,\sin\,\Omega\alpha)^2 \tag{5b}$$

and
$$\phi = \tan^{-1}\left(\frac{-d\Omega + \gamma\,\sin\,\Omega\alpha}{\omega_0^2 - \Omega^2 + \gamma\,\cos\,\Omega\alpha}\right). \tag{5c}$$

For sufficiently large values of Ω we can further approximate the solution (5) by dropping the terms ω_0^2 and $-d\Omega$. However, in our treatment we keep these terms in the solution. For a fixed value of γ the quantity μ varies periodically with α with period $2\pi/\Omega$. In the absence of time delay, $\mu \approx \Omega^2$. Solution (5) gives $\psi_{\mathrm{av}} = 0$, $\psi_{\mathrm{av}}^2 = g^2/(2\mu^2)$, and $\psi_{\mathrm{av}}^3 = 0$. Now Eq. (3) becomes

$$\ddot{X} + d\dot{X} + C_1 X + \beta X^3 + \gamma X(t-\alpha) = f\,\cos\,\omega t, \tag{6a}$$
where
$$C_1 = \omega_0^2 + \frac{3\beta g^2}{2\mu^2}. \tag{6b}$$

When $f = 0$, the equilibrium points of Eq. (6) are

$$X_0^* = 0, \qquad X_{\pm}^* = \pm\sqrt{-\frac{C_1 + \gamma}{\beta}}\;. \tag{7}$$

Slow oscillations occur around these equilibrium points. We treat g and α as control parameters. By varying these parameters, the number of equilibrium points and their stability can be changed for fixed values of other parameters.

Next, we consider the deviation Y of X from X^* and obtain

$$\ddot{Y} + d\dot{Y} + \omega_{\mathrm{r}}^2 Y + 3\beta Y^2 X^* + \beta Y^3 + \gamma Y(t-\alpha)$$
$$= f\,\cos\,\omega t, \tag{8a}$$
where
$$\omega_{\mathrm{r}}^2 = C_1 + 3\beta X^{*2}. \tag{8b}$$

For a weak input signal, i.e., $f \ll 1$, $|Y| \ll 1$ and hence we neglect the nonlinear terms in Eq. (8a). Then its solution in the limit $t \to \infty$ is $A_{\mathrm{L}}\,\cos(\omega t + \Phi)$, where $A_{\mathrm{L}} = f/\sqrt{S}$,

$$S = \left[\omega_{\mathrm{r}}^2 - (\omega^2 - \gamma\,\cos\,\omega\alpha)\right]^2 + [-d\omega + \gamma\,\sin\,\omega\alpha]^2 \tag{9}$$
and
$$\Phi = \tan^{-1}\left[\frac{-d\omega + \gamma\,\sin\,\omega\alpha}{\omega_{\mathrm{r}}^2 - (\omega^2 - \gamma\,\cos\,\omega\alpha)}\right]. \tag{10}$$

The response amplitude Q is A_{L}/f, i.e., $Q = 1/\sqrt{S}$, and ω_{r} is the resonant frequency of oscillation of the slow variable $X(t)$. An important observation from the theoretical expression of Q is that it has periodic dependence on α with two periods $2\pi/\omega$ and $2\pi/\Omega$. In the expression for Q the quantity ω_{r}^2 has a periodic dependence on α with period $2\pi/\Omega$. In Q, there are two other terms containing α and are oscillating around γ with period $2\pi/\omega$. There is no periodic term in Q for $\gamma = 0$. In the following, we analyze the occurrence of VR separately for the double-well and the single-well cases.

B. Resonance analysis in the double-well system

For $\omega_0^2 < 0$, $\beta > 0$, and $\gamma = 0$ the potential of the unforced and undamped system (1) is of a double-well form (Fig. 1). For simplicity we always choose the same sign for γ and ω_0^2. In the presence of damping, feedback, and biharmonic force the

equilibrium points around which slow oscillations take place are given by Eq. (7). There are three equilibrium points for $g < g_{\mathrm{c}}$, where

$$g_{\mathrm{c}} = \left[\frac{2\mu^2}{3\beta}\left(|\omega_0^2| + |\gamma|\right)\right]^{1/2}, \tag{11}$$

while for $g > g_{\mathrm{c}}$, X_0^* is the only real equilibrium point. That is, the effective potential of the slow variable X undergoes a transition from the double well to a single well at g_{c}.

The condition for the response amplitude Q to be maximum at a value of g is $dS/dg = 0$, where S is given by Eq. (9). We denote g_{VR} as the value of g at which the response amplitude Q becomes a maximum. An analytical expression for g_{VR} can be obtained from $dS/dg = 0$. The following results are obtained:
   Case 1. $|\gamma| < |\gamma_{\mathrm{c}}| = \omega^2/(1 - \cos\,\omega\alpha)$.

$$g_{\mathrm{VR}}^{(1)} = \left[\frac{\mu^2}{3\beta}\left(2|\omega_0^2| + 3|\gamma| - \omega^2 - |\gamma|\cos\,\omega\alpha\right)\right]^{1/2} < g_{\mathrm{c}}, \tag{12a}$$

$$g_{\mathrm{VR}}^{(2)} = \left[\frac{2\mu^2}{3\beta}\left(|\omega_0^2| + \omega^2 + |\gamma|\cos\,\omega\alpha\right)\right]^{1/2} > g_{\mathrm{c}}. \tag{12b}$$

Case 2. $|\gamma| > |\gamma_{\mathrm{c}}| = \omega^2/(1 - \cos\,\omega\alpha)$.

$$g_{\mathrm{VR}}^{(1)} = g_{\mathrm{c}}. \tag{13}$$

In case 1 a resonance occurs at two values of g, one at a value of $g < g_{\mathrm{c}}$, and another at a value of $g > g_{\mathrm{c}}$. The response amplitude is the same at these two values of g. In case 2 only one resonance is possible and it occurs at the bifurcation point g_{c}.

To verify our theoretical results, we compute the sine and cosine components Q_{s} and Q_{c}, respectively, at the low frequency ω of the numerical solution $x(t)$ of system (1). In the calculation of Q_{s} and Q_{c} the solution $x(t)$ corresponding to 200 drive cycles of the input signal after leaving a sufficient transient is used. Then, $Q = \sqrt{Q_{\mathrm{s}}^2 + Q_{\mathrm{c}}^2}/f$. Throughout our study we fix the values of the parameters as $d = 0.5$, $f = 0.1$, $\omega = 1$, and $\Omega = 10$. For the double-well case we choose $\omega_0^2 = -1$ and $\beta = 0.1$. Equation (1) is integrated numerically using the Euler method with time step 0.01. The time-delayed parameter α always takes multiple values of 0.01.

In the absence of time-delayed feedback ($\gamma = 0$), the double-well system (1) exhibits two resonances for $2|\omega_0^2| > \omega^2$ and one for $2|\omega_0^2| < \omega^2$. For $\gamma \neq 0$ the resonance condition is independent of ω_0^2 and depends on the parameters ω, γ, and α. Even for $2|\omega_0^2| < \omega^2$ for a range of values γ and α the system can be induced to show a double resonance. Figure 2(a) presents both theoretical and numerical g_{VR} as a function of γ for $\alpha = 1$ and 3. Very good agreement is found between the theory and the numerical simulation. For $\alpha = 1$ and 3, the values of γ_{c} are $-2.175\,34$ and $-0.502\,51$, respectively. There are two resonances for $|\gamma| < |\gamma_{\mathrm{c}}|$ and only one for $|\gamma| > |\gamma_{\mathrm{c}}|$. For $|\gamma| < |\gamma_{\mathrm{c}}|$, as g increases from 0, two stable slow oscillations take place around X_+^* and X_-^*. ω_{r}^2 decreases from $2|\omega_0^2| + 3|\gamma|$ and reaches the minimum value $|\gamma|$ at $g = g_{\mathrm{c}}$. For $g > g_{\mathrm{c}}$ there is only one stable slow motion and is around $X_0^* = 0$. As g increases from g_{c} the value of ω_{r}^2
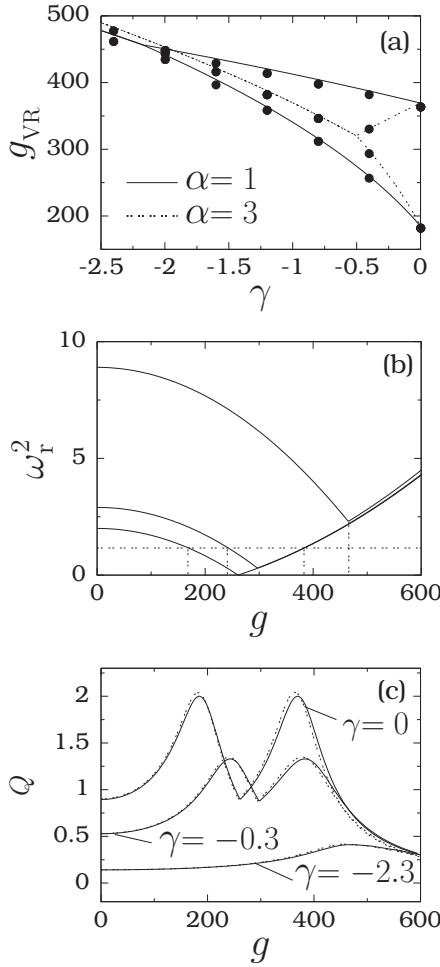
FIG. 2. (a) Theoretical and numerical g_{VR} versus the parameter γ for two fixed values of the time-delayed parameter γ for the underdamped system (1) with the double-well potential case. The solid circles are the numerically computed g_{VR} and the lines are theoretical g_{VR}. The values of the parameters are $d = 0.5$, $\omega_0^2 = -1$, $\beta = 0.1$, $f = 0.1$, $\omega = 1$, and $\Omega = 10$. (b) The variation of theoretical ω_r^2 with parameter g. From bottom to top, the curves show the values of γ are 0, -0.3, and -2.3, respectively. The horizontal dashed line represents the value of $(\omega^2 - \gamma \cos \omega\alpha)$. The vertical dashed lines mark the values of g_{VR}. (c) Plot of the response amplitude Q as a function of g for $\gamma = 0$, -0.3, and -2.3 with $\alpha = 1$. The continuous lines are theoretical Q, while the dashed lines are numerically calculated Q.

increases continuously from the value $|\gamma|$. This is shown in Fig. 2(b) for $\gamma = 0$, -0.3, and -2.3. For $\gamma = 0$ and -0.3 at two values of g, namely, at $g_{VR}^{(1)}$ and $g_{VR}^{(2)}$, $\omega_r^2 = \omega^2 - \gamma \cos \omega\alpha$ [indicated by the horizontal dashed line in Fig. 2(b)], and hence Q becomes maximum with $Q_{max} = 1/| - d\omega + \gamma \sin \omega\alpha|$. In Fig. 2(c) we notice the appearance of two resonances. In the absence of time-delayed feedback Q becomes maximum when $\omega_r = \omega$ and the maximum value of Q is $1/(d\omega)$. For $\gamma = -0.3$ the theoretical values of $g_{VR}^{(1)}$ and $g_{VR}^{(2)}$ are 242.75 and 382.95, while the numerically computed values are 240.34 and 377.43, respectively.

For $|\gamma| > |\gamma_c|$ the value of ω_r^2 is always $> (\omega^2 - \gamma \cos \omega\alpha)$. However, it has a local minimum at $g = g_c$, and thus there occurs a resonance. These are shown in Figs. 2(b) and 2(c) for
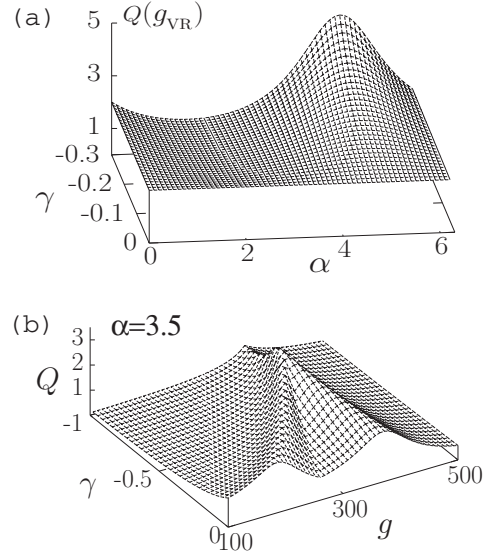
FIG. 3. (a) Variation of the maximum value of Q, $Q(g = g_{VR})$, as a function of γ and α for the double-well underdamped system. (b) Three-dimensional plot of Q versus the parameters γ and g for $\alpha = 3.5$.

$\gamma = -2.3$. The noteworthy observation is that for $|\gamma| < |\gamma_c|$ the double resonance is due to matching of ω_r^2 with $\omega^2 - \gamma \cos \omega\alpha$, while the single resonance for $|\gamma| > |\gamma_c|$ is due to the local minimization of ω_r^2. The single resonance always occurs at $g = g_c$ at which the effective potential of the slow variable undergoes a transition from the double well to a single well. Note that Q is minimum at $g = g_c$ for $|\gamma| < |\gamma_c|$.

In Fig. 2(c), for $\alpha = 1$ the maximum value of the response amplitude is always lower than the case $\gamma = 0$. $Q_{max}(\gamma, g) = Q(\gamma, g_{VR}) > Q(\gamma = 0, g_{VR})$ can be realized for a range of values of α and γ, particularly for $|\gamma| < |\gamma_c|$ and $\alpha \in [(2n - 1)\pi/\omega, 2n\pi/\omega]$, $n = 1, 2, \ldots$. Figure 3(a) shows the variation of $Q(g_{VR})$ in (γ, α) parameter space for $\alpha \in [0, 2\pi]$ with $\omega = 1$. We can clearly see that $Q(\gamma, g_{VR}) > Q(\gamma = 0, g_{VR})$ for $\alpha \in [\pi, 2\pi]$. Figure 3(b) is the three-dimensional plot of Q as a function of γ and g for $\alpha = 3.5$. For $\alpha = 3.5$ the value of γ_c is 0.51641. In Fig. 3(b), for $|\gamma| < 0.51641$ we notice two resonances and further $Q(\gamma, g_{VR}) > Q(\gamma = 0, g_{VR})$. Only one resonance occurs for $|\gamma| > 0.51641$.

We compare the change in the slow motion $X(t)$ and the actual motion $x(t)$ when the parameter g is varied. For $\gamma = -0.3$ and $\alpha = 1$, when g is increased resonance occurs at two values of g. The numerically calculated values of g_{VR} are 240.5 and 376.85. In Fig. 4 the phase portrait of the slow motion $X(t)$ is plotted for several values of g. For $g < g_c$ (= 296.95) two slow motions occur: one around X_+^* and another around X_-^*. As g increases from a small value the equilibrium points about which $X(t)$ and $x(t)$ occur move toward the origin. This is shown in Fig. 4 for four values of $g < g_c$. For clarity, the orbits coexisting for $X < 0$ are not shown. For $g > g_c$ there is only one equilibrium point X_0^* and it does not move with an increase in g. Consequently, the slow orbit $X(t)$ and the actual orbit $x(t)$ occur around the origin. This is illustrated in Fig. 4 for three values of $g > g_c$. We point out that at the resonance value $g = 240.50$ there is no cross-well motion of
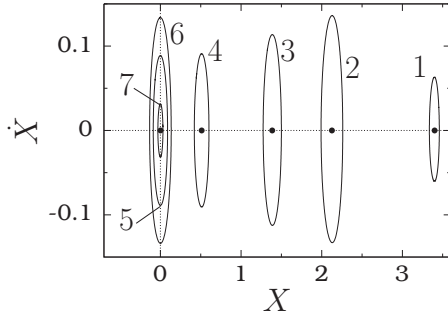
FIG. 4. Phase portraits of the slow motion of the underdamped double-well system for several values of g. The values of g for the numbers 1–7 are 100 (1), 240.5 (2), 275 (3), 295 (4), 300 (5), 376.85 (6), and 600 (7). The values of other parameters are $d = 0.5$, $\omega_0^2 = -1$, $\beta = 0.1$, $\gamma = -0.3$, $\alpha = 1$, $f = 0.1$, $\omega = 1$, and $\Omega = 10$. The solid circles mark the equilibrium points X_0^* and X_+^*.

$X(t)$ or $x(t)$; that is, cross-well motion and bistability are not necessary ingredients for VR. As a matter of fact, it can occur in monostable systems [9].

The condition for a resonance to occur when the time-delayed parameter α is varied is given by (from $dS/d\alpha = 0$)

$$\left(\omega_r^2 - \omega^2\right)\omega_{r\alpha}^2 + \left(\omega_{r\alpha}^2 - d\omega^2\right)\gamma \cos \omega\alpha$$
$$-\gamma\omega\left(\omega_r^2 - \omega^2\right)\sin \omega\alpha = 0, \qquad (14)$$

where $\omega_{r\alpha}^2 = d\omega_r^2/d\alpha$. Analytical expressions for the roots of the above equation are difficult to obtain. However, the roots denoted as α_{VR} can be determined numerically from Eq. (14). We computed theoretical α_{VR} [from Eq. (14)] and numerical α_{VR} [by numerically solving Eq. (1)] for a range of values of g with $\gamma = -0.3$. In Fig. 5(a) $\alpha_{VR} < 3 \times 2\pi/\omega$ are alone plotted (α_{VR} are periodic with period $2\pi/\omega$). In our study $\Omega \gg \omega$. For $\omega = 1$ and $\Omega = 10$, the ratio $\Omega/\omega = 10$ is a rational number. The response amplitude Q is thus periodic in α with period $2\pi/\omega$. This is because the solution of system (1) is periodic with respect to α with period $2\pi/\omega$. Suppose there are m values of α_{VR} in the interval $[0, 2\pi/\omega]$. Then the other values of $\alpha_{VR} > 2\pi/\omega$ are given by

$$\alpha_{VR}^{(i+jm)} = \alpha_{VR}^{(i)} + j\frac{2\pi}{\omega}, \quad i = 1, 2, \ldots, m, \quad j = 1, 2, \ldots. \tag{15}$$

Figure 5(b) presents numerical Q as a function of α and g. We can clearly see the periodicity of Q with respect to the time-delayed parameter α. We note that when g is varied, since in the expression for A_L or S only ω_r^2 depends on g, the variation of S is due to the variation of ω_r^2, and as pointed out earlier, the resonance is due to either the matching of ω_r^2 with $\omega^2 - \gamma \cos \omega\alpha$ or local minimization of ω_r^2. In contrast to this, then the delay parameter α is varied, not only ω_r^2 varies, but two other terms in S also vary with α. Consequently, the resonance is due to the local minimization of the quantity S.

Figure 6 shows the effect of α on the slow motion $X(t)$ for $g = 250$ and 350. For fixed values of the parameters when α is varied the equilibrium point around which slow orbit occurs depends on the value of g. If $g < g_c$, then the slow orbits about $X_\pm^*$ are stable. When α is varied the shift in the locations of $X_\pm^*$ is very small. However, the amplitude of the slow orbits vary
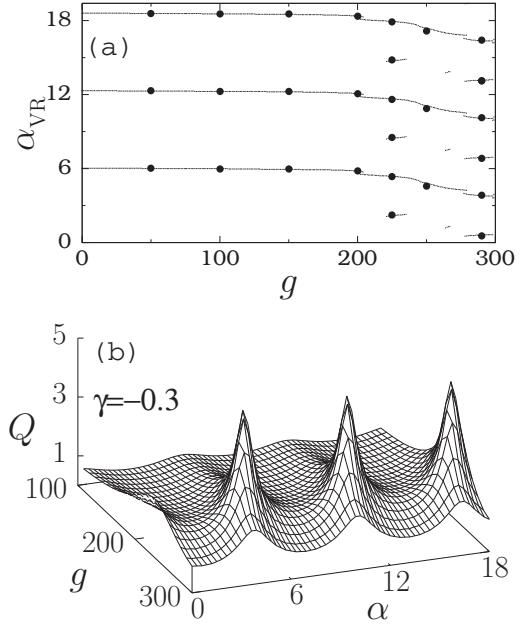
FIG. 5. (a) α_{VR} versus the amplitude g of the high frequency force for $\gamma = -0.3$. The system is the underdamped double-well system. Continuous lines and solid circles represent theoretically and numerically computed values of α_{VR}, respectively. (b) Periodic variation of the response amplitude Q with the time-delayed parameter α for various values of g in the interval $[100, 300]$ for $\gamma = -0.3$.

and resonance occurs at $\alpha = \alpha_{VR}$. When g is fixed at a value $> g_c$ and α is varied, the slow orbit occurs about $X_0^* = 0$. These are shown in Fig. 6 for $g = 250 < g_c$ and $g = 350 > g_c$. For $g = 250 (< g_c)$ the slow motion occurs at about X_+^* and X_-^*. This is shown in Figs. 6(a) and 6(b) for a few values of α. In these figures the resonant orbits are marked by the label "2."
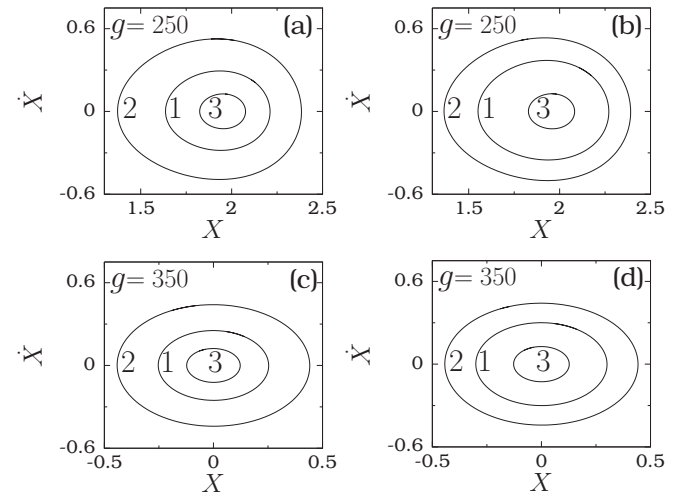
FIG. 6. Phase portraits of the slow orbit as a function of the time-delayed parameter $\alpha (\leqslant 14)$ for two fixed values of g. (a) $g = 250$, $\alpha = 4$ (1), 4.57 (2), and 8 (3). (b) $g = 250$, $\alpha = 10.5$ (1), 10.97 (2), and 14 (3). (c) $g = 350$, $\alpha = 3.5$ (1), 4.41 (2), and 7 (3). (d) $g = 350$, $\alpha = 10$ (1), 10.69 (2), and 13 (3). In the numerical simulation resonance is observed at $\alpha = 4.57$ and 10.97 for $g = 250$ and at $\alpha = 4.41$ and 10.69 for $g = 350$.

The orbits marked by "1" and "3" correspond to the values of α on either side of $\alpha = \alpha_{VR}$. In Figs. 6(c) and 6(d), for $g = 350 > g_c$, slow motion occurs at about $X_0^* = 0$. Tuning time delay is an advantage when it is desired to observe the response of a system and VR with the center of the orbit (slow as well as the actual orbit) almost remaining the same.

C. Resonance analysis in the single-well system

For $\omega_0^2, \beta > 0$ the potential $V(x)$ has a single-well shape with a local minimum at $x = 0$. Unlike the double-well system, the effective potential of the slow variable X remains as a single well when the parameter g is varied. The equilibrium point around which slow oscillation occurs remains as $X_0^* = 0$.

The resonance value of g, g_{VR}, is given by

$$g_{VR} = \left[\frac{2\mu^2}{3\beta} \left(\omega^2 - \gamma \, \cos \, \omega\alpha - \omega_0^2 \right) \right]^{1/2} \quad (16a)$$

provided

$$\omega^2 - \gamma \, \cos \, \omega\alpha > \omega_0^2. \quad (16b)$$

In the double-well system a resonance is possible for all sets of values of γ and α when g is varied. In contrast to this, in the single-well case a resonance is possible only for a set of values of γ and α for which the condition (16b) is satisfied. Further, in the double-well system two resonances are possible, while in the single-well system, at most one resonance is possible. The theoretical approach considered in the present work helps us to choose appropriate values of the parameters to realize VR.

Figure 7(a) shows the variation of theoretical g_{VR} with γ and $\alpha \in [0, 2\pi/\omega]$ for $\omega_0^2 = 0.5$ and $\beta = 0.1$. For a fixed value of γ, as α increases from zero the value of g_{VR} increases and becomes maximum at $\alpha = \pi/\omega$ and then decreases. This is clear from Eq. (16a). g_{VR} is periodic in α with period $2\pi/\omega$ and $Q_{max} = 1/| -d\omega + \gamma \, \sin \, \omega\alpha |$.

(a)

(b)
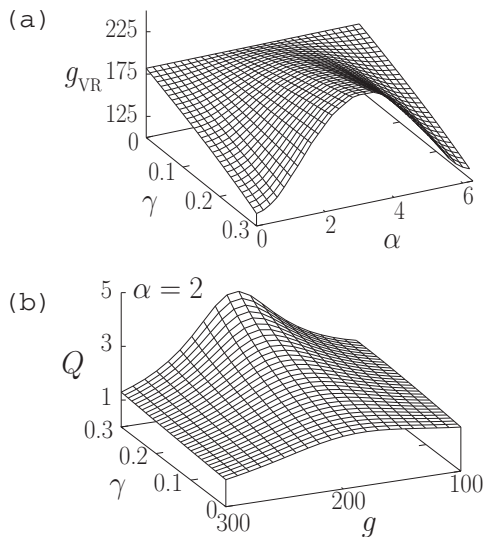
FIG. 7. (a) Theoretical g_{VR} versus the time-delayed feedback parameters γ and α for the underdamped single-well system with $\omega_0^2 = 0.5$ and $\beta = 0.1$. (b) Q versus the parameters γ and g for $\alpha = 2$.
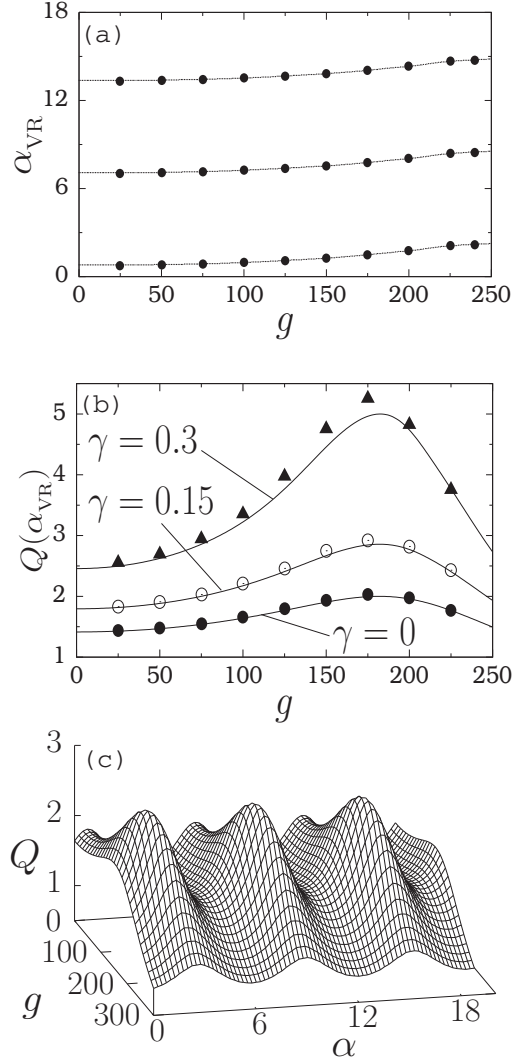
FIG. 8. (a) α_{VR} versus g for $\gamma = 0.15$. The system is the underdamped single-well system. Continuous lines and solid circles represent theoretically predicted and numerically calculated values of α_{VR}, respectively. Here $d = 0.5$, $\omega_0^2 = 0.5$, $\beta = 0.1$, $\gamma = 0.15$, $f = 0.1$, $\omega = 1$, and $\Omega = 10$. (b) Variation of $Q(\alpha_{VR})$ with g for $\gamma = 0.15$ and 0.3. Q versus g for $\gamma = 0$ is also shown. The continuous lines and symbols represent theoretically and numerically predicted values of Q. (c) Periodic variation of Q with the time-delayed parameter α for various values of g for $\gamma = 0.15$.

In Fig. 7(b) the maximum value of Q at $g = g_{VR}$ for $\alpha = 2$ increases when γ increases. In the single-well system a resonance also occurs when $\omega_r^2 = \omega^2 - \gamma \, \cos \, \omega\alpha$. For a certain range of values of α, g_{VR} decreases when γ increases, and moreover, the value of Q at resonance increases. For example, when $\alpha = 1$ the value of g_{VR} decreases when the value of γ increases. For $\alpha = 2$ and 3, g_{VR} increases when γ increases.

Figure 8(a) shows both theoretical and numerical α_{VR} versus g for $\gamma = 0.15$. α_{VR} is periodic with period $2\pi/\omega$. For $\alpha \in [0, 2\pi/\omega]$, resonance occurs at only one value of α for fixed values of g. In Fig. 5(a), corresponding to the double-well system, a double resonance is found for a certain range of fixed values of g. The presence of only one resonance in Fig. 8(a)
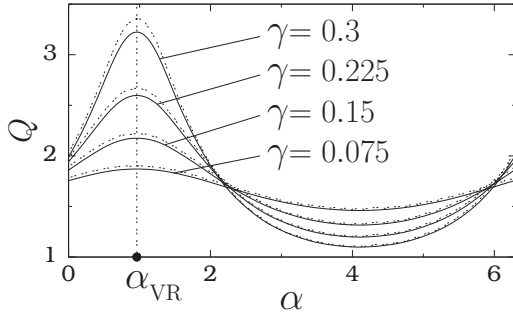
FIG. 9. Response amplitude Q versus the time-delayed parameter α for a few fixed values of γ and $g = 100$ for the underdamped single-well system. The continuous and dashed lines represent theoretically and numerically predicted values of Q, respectively. The vertical dashed line marks the value of α_{VR} given by Eq. (17).

for $\alpha \in [0, 2\pi/\omega]$ implies that the variation of μ^2 due to the terms $\gamma \sin \Omega\alpha$ and $\gamma \cos \Omega\alpha$ [see Eq. (5b)] is negligible and μ^2 can be approximated as $\mu^2 \approx (\omega_0^2 - \Omega^2)^2 + d^2\Omega^2$. Then from Eq. (9) the expression for α_{VR} is obtained as

$$\alpha_{\mathrm{VR}} = \frac{1}{\omega} \tan^{-1}\left(\frac{d\omega}{\omega^2 - \omega_{\mathrm{r}}^2}\right), \quad \omega_{\mathrm{r}}^2 = C_1 \qquad (17)$$

and is independent of γ. This is confirmed by numerical simulation. In Fig. 9, Q versus α is plotted for $g = 100$ and for a few fixed values of γ. Q is maximum at the same value of α, however, its maximum value at resonance varies with γ. Figure 8(b) shows the dependence of maximum value of Q at $\alpha = \alpha_{\mathrm{VR}}$ with the parameters g and γ. For each fixed value of γ the value of $Q(\alpha_{\mathrm{VR}})$ increases with g, becomes a maximum at a higher value of g, and then decreases. In Fig. 8(b) the maximum value of Q for $\gamma \neq 0$ is always greater than the value of Q for $\gamma = 0$. Figure 8(c) demonstrates the periodic variation of Q with the delay parameter α.

III. OVERDAMPED DUFFING OSCILLATOR

In this section we analyze the occurrence of VR in the overdamped system (2) with time-delayed feedback.

A. Theoretical approach

For system (2) the equation of motion for the slow variable X is

$$\dot{X} + C_1 X + \beta X^3 + \gamma X(t - \alpha) = f \cos \omega t, \qquad (18a)$$

where

$$C_1 = \omega_0^2 + \frac{3\beta g^2}{2\mu^2}, \qquad (18b)$$

$$\mu^2 = \left(\omega_0^2 + \gamma \cos \Omega\alpha\right)^2 + (-\Omega + \gamma \sin \Omega\alpha)^2. \qquad (18c)$$

The fast variable $\psi(\tau)$ is approximated as

$$\psi = \frac{g}{\mu} \cos(\tau + \phi),$$
$$\phi = \tan^{-1}\left[\frac{-\Omega + \gamma \sin \Omega\alpha}{\omega_0^2 + \gamma \cos \Omega\alpha}\right]. \qquad (19)$$

The equilibrium points around which slow motion occurs are again given by Eq. (7). The long time solution of the deviation $Y(t)$ of $X(t)$ from X^* is obtained as

$$Y(t) = A_{\mathrm{L}} \cos(\omega t + \Phi), \qquad (20a)$$

where

$$A_{\mathrm{L}} = \frac{f}{\sqrt{S}}, \quad \Phi = \tan^{-1}\left[\frac{-\omega + \gamma \sin \omega\alpha}{\omega_{\mathrm{r}}^2 + \gamma \cos \omega\alpha}\right], \quad (20b)$$

$$S = \left(\omega_{\mathrm{r}}^2 + \gamma \cos \omega\alpha\right)^2 + (-\omega + \gamma \sin \omega\alpha)^2, \quad (20c)$$

$$\omega_{\mathrm{r}}^2 = C_1 + 3\beta X^{*2}. \qquad (20d)$$

The response amplitude Q is $1/\sqrt{S}$. The expression for the function S given by Eq. (20c) for the overdamped system can be compared with that of the underdamped system given by Eq. (9).

B. Double-well case

For $\omega_0^2 < 0$, $\gamma < 0$, $\beta > 0$ the critical value of g, g_{c}, below which three equilibrium points X_0^*, $X_{\pm}^*$ exist and above which only one equilibrium point X_0^* exists is again given by Eq. (11) with μ^2 given by Eq. (18c).

Suppose we vary g from zero. From the theoretical expression of Q (or S) the condition for Q to be maximum is $\omega_{\mathrm{r}}^2 - |\gamma| \cos \omega\alpha = 0$. In the absence of time delay ($\gamma = 0$) resonance occurs when $\omega_{\mathrm{r}}^2 = 0$. For $\gamma \neq 0$ and $g < g_{\mathrm{c}}$ the slow motion is about $X_{\pm}^*$ and

$$\omega_{\mathrm{r}}^2 = 2|\omega_0^2| + 3|\gamma| - \frac{3\beta g^2}{\mu^2}$$
$$= |\gamma| + \frac{3\beta}{\mu^2}\left(g_{\mathrm{c}}^2 - g^2\right), \quad g < g_{\mathrm{c}}, \qquad (21)$$

while for $g > g_{\mathrm{c}}$ it is about $X_0^* = 0$ and

$$\omega_{\mathrm{r}}^2 = -|\omega_0^2| + \frac{3\beta g^2}{2\mu^2}$$
$$= |\gamma| + \frac{3\beta}{2\mu^2}\left(g^2 - g_{\mathrm{c}}^2\right), \quad g > g_{\mathrm{c}}. \qquad (22)$$

As g increases from zero, the value of ω_{r}^2 decreases from $2|\omega_0^2| + 3|\gamma|$, becomes $|\gamma|$ at $g = g_{\mathrm{c}}$, and increases from $|\gamma|$ with a further increase in g. ω_{r}^2 is always $\geqslant |\gamma|$. That is, $\omega_{\mathrm{r}}^2 - |\gamma| \cos \omega\alpha$ never becomes zero except when $\alpha = 2n\pi/\omega$, $n = 0, 1, 2, \ldots$ and $g = g_{\mathrm{c}}$. For all other values of α, even though $\omega_{\mathrm{r}}^2 - |\gamma| \cos \omega\alpha$ does not vanish, this quantity becomes a minimum at $g = g_{\mathrm{c}}$, and hence a resonance at $g_{\mathrm{VR}} = g_{\mathrm{c}}$. We recall that in the underdamped delay-feedback system $g_{\mathrm{VR}} = g_{\mathrm{c}}$ only if $|\gamma| > |\gamma_{\mathrm{c}}| = \omega^2/(1 - \cos \omega\alpha)$.

Figure 10(a) shows the variation of theoretical g_{VR} with the delay parameters γ and α for $\omega_0^2 = -1$ and $\beta = 1$. g_{VR} oscillates with α for each fixed value of γ. On the other hand, for a fixed value of α the value of g_{VR} increases with an increase in $|\gamma|$. For the values of γ and α in Fig. 10(b) we notice $Q(\gamma, \alpha, g_{\mathrm{VR}}) > Q(\gamma = 0, g_{\mathrm{VR}})$. For $\alpha = 6$ and $\gamma = 0$, -1, and -2 the theoretical values of g_{VR} are 8.2, 11.2, and 13.34 respectively. Numerically calculated values of g_{VR} are 8.24, 10.98, and 13.34 respectively. The theoretical g_{VR} values are in close agreement with numerical g_{VR}. The variation of the response amplitude Q with g and γ is shown in Fig. 10(c),
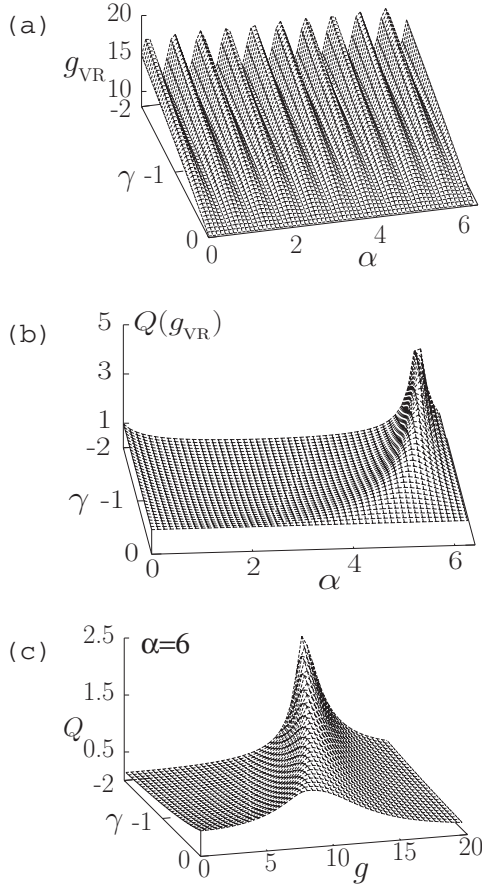
FIG. 10. Theoretically predicted (a) g_{VR} as a function of γ and α for the overdamped double-well system with $\omega_0^2 = -1$, $\beta = 1$, $f = 0.1$, $\omega = 1$, and $\Omega = 10$, (b) $Q(g_{VR})$ versus the parameters γ and α, and (c) variation of the response amplitude Q with γ and g for $\alpha = 6$.

where $\alpha = 6$. The maximum value of Q increases with an increase in $|\gamma|$. The response of the system is greatly enhanced by the delay feedback.

Next, we consider the effect of α with $\omega = 1$ and $\Omega = 10$. Figure 11 shows α_{VR} versus g for $\gamma = -1$. In this figure α_{VR} in the interval $[0, 2\pi/\omega]$ alone are plotted. If resonance occurs at a value of $\alpha_{VR} < 2\pi/\omega$, then it occurs at $\alpha_{VR} + 2n\pi/\omega$, $n = 1, 2, \ldots$ also. We consider the interval $\alpha \in [0, 2\pi/\omega]$. For small values of g there is only one value of α_{VR}. An example is given in Fig. 12(a) for $g = 1$. We note that $Q(\alpha_{VR}) \approx Q(\gamma = 0)$, i.e., Q is not improved considerably. The number of values of α_{VR} increases with an increase in g. In Fig. 12(b), corresponding to $g = 8$, we can clearly see multiple resonance. Resonance occurs at ten values of α_{VR} (in the interval $[0, 2\pi/\omega]$). [However, $Q(\alpha_{VR}) > Q(\gamma = 0)$ is found only at a few values of α_{VR}]. The response amplitude profile repeats in every $2\pi/\omega$ intervals of α.

For $g = 12$ [Fig. 12(c)] the number of resonances is doubled. At certain values of α_{VR} the value of Q is considerably larger than $Q(\gamma = 0)$. The enhancement of Q is reduced for higher values of g as shown in Fig. 12(d) for $g = 20$. Above certain fixed values of g the resonance curve is modulated by the high frequency signal. The modulation period is not strictly $2\pi/\Omega$. For $g = 1, 2, 5, 12$, and 15 the
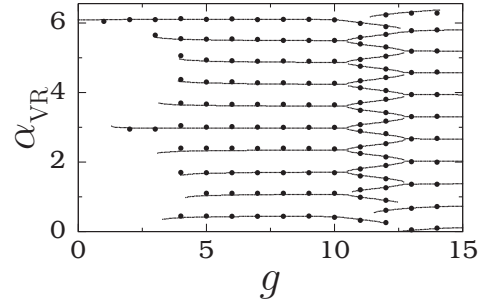
FIG. 11. α_{VR} versus g for the overdamped double-well system with $\gamma = -1$. Continuous lines and solid circles represent theoretical and numerical values of α_{VR}, respectively.

number of resonances are 1, 2, 10, 20, and 10, respectively. The complicated dependence of the number of resonances and the spacing between the consecutive α_{VR}'s is due to the complicated dependence of S with the delay parameters γ and α. The maximum value of Q increases when g increases, and for higher values of g it decreases.

For irrational values of the ratio Ω/ω the response amplitude exhibits a quasiperiodic pattern. An example is presented
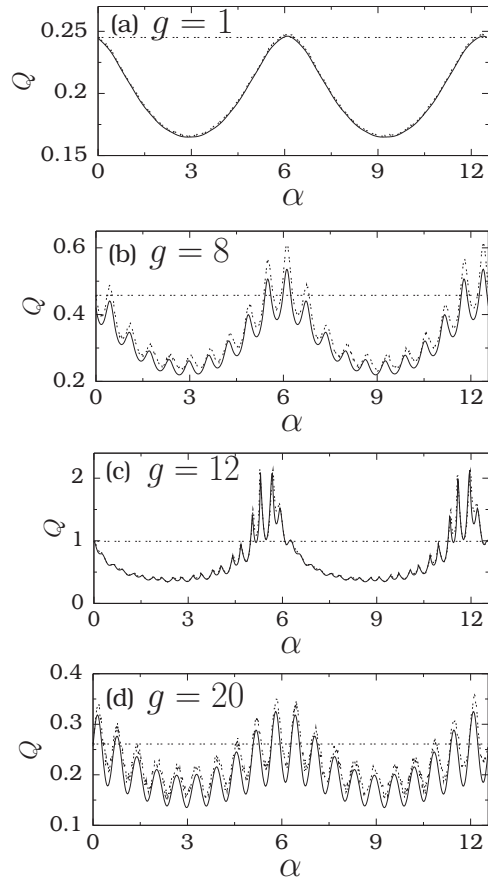
FIG. 12. Theoretical (represented by continuous lines) and numerical (represented by dashed lines) Q as a function of the delay parameter α for four fixed values of the parameter g. The system is the double-well overdamped system with $\gamma = -1$. The horizontal dashed line denotes the value of Q in the absence of time-delayed feedback.
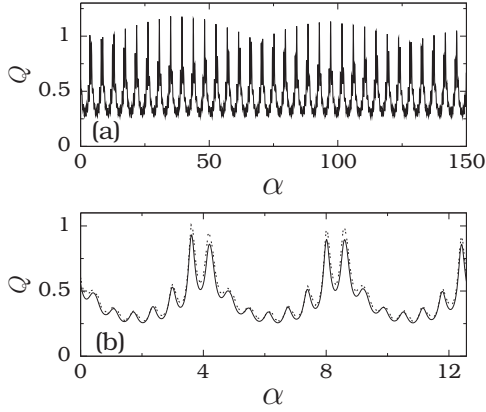
FIG. 13. (a) Quasiperiodic variation of Q with the delay parameter α for $\omega = \sqrt{2}$, $\Omega = 10$, and $g = 10$. The system is the overdamped double-well system. (b) Enlargement of part (a). Continuous and dashed lines represent the theoretically and numerically calculated values of Q, respectively.

in Fig. 13 for $\omega = \sqrt{2}$, $\Omega = 10$, and $g = 10$. The maximum values of Q in every $2\pi/\omega$ interval of α are not the same. Further, $\alpha_{\text{VR}} \neq \alpha'_{\text{VR}} + 2n\pi/\omega, n = 1, 2, \ldots$ where α'_{VR} is a value of α_{VR} in the interval $[0, 2\pi/\omega]$.

C. Single-well system

Finally, we consider the overdamped single-well system. Since $X_0^* = 0$ is the only equilibrium point around which slow motion occurs, we have $\omega_r^2 = C_1$, and it increases monotonically from ω_0^2 when g increases.

g_{VR} is given by

$$g_{\text{VR}} = \left[\frac{2\mu^2}{3\beta} \left(-\omega_0^2 + \gamma |\cos \omega\alpha| \right) \right]^{1/2}, \qquad (23a)$$

where

$$\alpha \in \left[\left(2n + \frac{1}{2} \right) \frac{\pi}{\omega}, \left(2n + \frac{3}{2} \right) \frac{\pi}{\omega} \right], \quad n = 0, 1, \ldots \quad (23b)$$

and

$$\gamma > \gamma_c = \frac{\omega_0^2}{|\cos \omega\alpha|}. \qquad (23c)$$

In the double-well system there is no restriction on the values of ω_0^2, ω, α, and γ for resonance when g is varied. In the single-well system a resonance at a value of g given by Eq. (23a) occurs only for the parametric restrictions given by Eqs. (23b) and (23c). An important observation from Eq. (23a) is that in the absence of time delay the single-well system cannot exhibit a resonance when g (or Ω) is varied, and Q decreases continuously with an increase in g. But resonance can be induced by an appropriate time-delayed feedback.

Variation of theoretical g_{VR} with the delay parameters γ and α is depicted in Fig. 14(a) for $\omega_0^2 = 0.8$ and $\beta = 1$. The effect of α and γ on g_{VR} can be clearly seen. In Fig. 14(b) a comparison of theoretical g_{VR} with numerical g_{VR} is made for a range of values of γ for three fixed values of α. Similar to the other systems for the single-well overdamped system it is also difficult to obtain an analytical expression for α_{VR}. Figure 15 presents both theoretically predicted and numerically computed values of $\alpha_{\text{VR}} \in [0, 2\pi/\omega]$ for a range of values of g with $\gamma = 1$. The theoretical prediction is in close
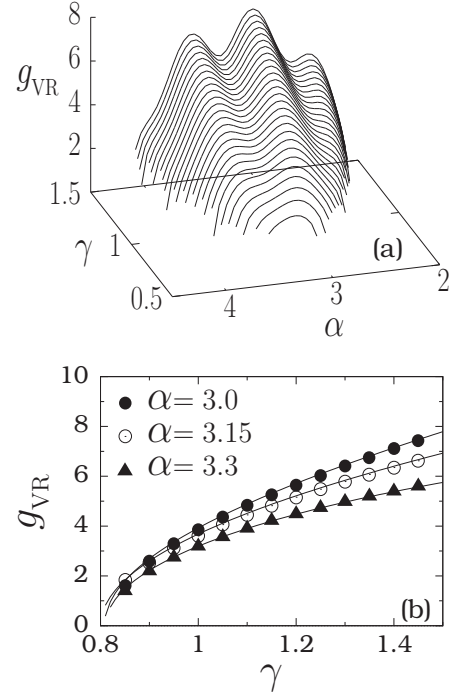
FIG. 14. (a) Theoretically predicted g_{VR} versus the delay parameters γ and α for the single-well overdamped system. The values of other parameters are $\omega_0^2 = 0.8$, $\beta = 1$, $f = 0.1$, $\omega = 1$, and $\Omega = 10$. (b) g_{VR} versus γ for three fixed values of α. Continuous lines are theoretical g_{VR}, while the symbols represent numerically computed values of g_{VR}.

agreement with the numerical simulation. In Fig. 16, Q versus α is shown. In this system also, $Q(\alpha)$ is periodic in α with period $2\pi/\omega$ for rational values of Ω/ω and quasiperiodic for irrational values of Ω/ω. In the interval $\alpha \in [0, 2\pi/\omega]$ single resonance occurs for small values of g (as shown in Fig. 16 for $g = 3$). Multiple resonance occurs for higher values of g. This is shown in Fig. 16 for $g = 5$ and 8. $Q(\alpha = \alpha_{\text{VR}})$ decreases with an increase in g. For $g = 3$, 5, and 8 the number of resonances in the interval $0 < \alpha < 2\pi/\omega$ are 1, 4, and 10, respectively.

IV. VALIDITY OF THEORETICAL APPROACH

It is important to analyze the validity of the theoretical approach used in the present work on VR. This is because the systems considered here are capable of exhibiting various
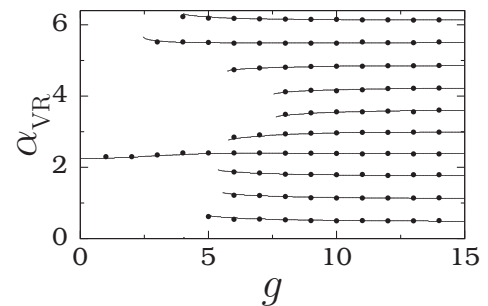
FIG. 15. Plot of theoretical α_{VR} (represented by continuous lines) and numerical α_{VR} (solid circles) versus g for $\gamma = 1$. The system is the single-well overdamped system.
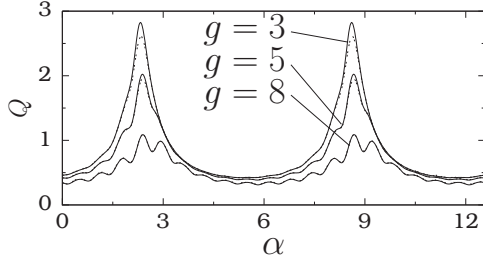
FIG. 16. Response amplitude Q as a function of the delay parameter α for three fixed values of g for the overdamped single-well system. Theoretical and numerical values of Q are represented by continuous and dashed lines, respectively. The dashed lines are not visible for $g = 5$ and 8 because of the very closeness of theoretical Q with the numerical Q.

bifurcation phenomena and chaotic motion. In this connection we note that as pointed out by Blekhman and Landa [5] and Chizhevsky [6] the dynamics of the slow variable X is highly sensitive to external perturbations for parametric values near the transition from one type of stability to another type, for example, bistability to monostability. In system (1) with the double-well case, as the control parameter g is varied, the effective potential V_{eff} changes from double well to a single well at $g = g_c$, given by Eq. (11). For values of g near g_c considerable deviation of theoretical Q from numerical Q is found. We numerically study the effect of the parameters ω, γ, α, and d for a range of values of g on theoretical Q in both double-well and single-well systems.

For $d = 0.5$, $\omega_0^2 = -1$, $\beta = 0.1$, $\gamma = -0.3$, $\alpha = 1$, and $\Omega = 10$ the value of g_c is 296.94. Figure 17(a) shows ω versus Q for three values of g near g_c. For $g = 250$ and 350, far before and far after the bifurcation point g_c, respectively, theoretical Q is in good agreement with numerical Q even for small values of
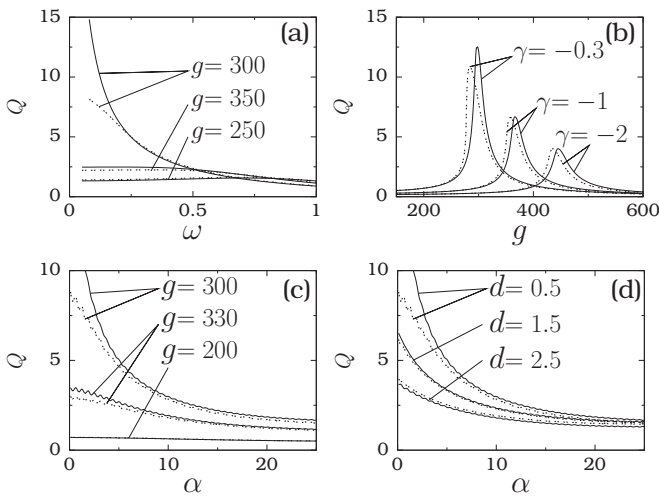
FIG. 17. (a) ω versus theoretical Q (marked by continuous lines) and numerical Q (marked by dashed lines) for three values of g for system (1) with double-well potential. Here $d = 0.5$, $\omega_0^2 = -1$, $\beta = 0.1$, $\gamma = -0.3$, $\alpha = 1$, $\Omega = 10$, and $f = 0.1$. (b) g versus Q for three values of γ with $\omega = 0.1$. [(c),(d)] α versus Q. (c) $\omega = 0.1$, $\gamma = -0.3$, and $d = 0.5$. (d) $\omega = 0.1$, $\gamma = -0.3$, and $g = 300$.
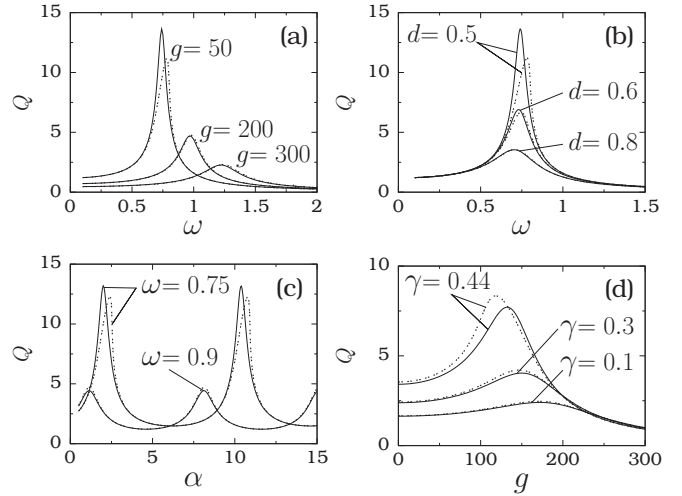
FIG. 18. (a) ω versus theoretical Q (marked by continuous lines) and numerical Q (marked by dashed lines) for three values of g for the system (1) with a single-well potential. Here $d = 0.5$, $\omega_0^2 = 0.5$, $\beta = 0.1$, $\gamma = 0.3$, $\alpha = 1$, $\Omega = 10$, and $f = 0.1$. (b) ω versus Q for three values of d with $g = 50$. (c) α versus Q for two values of ω with $g = 50$ and $d = 0.5$. (d) g versus Q for three values of γ with $\alpha = 1$, $\omega = 1$, and $d = 0.5$.

ω. For $g = 300$, a value close to g_c, the deviation of theoretical Q from numerical Q is large for small values of ω. In Fig. 17(b) we plotted g versus Q at $\omega = 0.1$ for three values of γ. For $\gamma = -0.3$, -1, and -2 the values of g_c are 296.94, 366.10, and 444.53, respectively. We can clearly notice a discrepancy between the theoretical and numerical values of g near g_c. The values of two Q's are close to each other for the values of g far away from g_c. The effect of α is shown in Fig. 17(c). The deviation between theoretical Q and numerical Q is large for a range of values of α when $g = 300$. For two other values of g, namely, $g = 200$ and 330, the theoretical result is close to the numerical result. The deviation between theory and numerical simulation can be reduced by increasing the value of the damping coefficient d. This is shown in Fig. 17(d). An important observation from Figs. 17(a)–17(d) is that the deviation of theoretical Q from numerical Q is considerably large near the bifurcation point g_c, and the deviation can be reduced by increasing the damping parameter d.

What do we observe in the single-well case of system (1) where V_{eff} remains monostable when the parameter g is varied? Figure 18 summarizes the effect of various parameters on Q. A common feature we notice in Figs. 17 and 18 is that when both theoretical Q and numerical Q values are roughly < 3 we observe close agreement between theory and numerical simulation. Therefore, we point out that in practical applications of the theoretical treatment of VR it is appropriate to avoid the parameters values for which $Q_{\text{max}} \gg 1$.

V. CONCLUSIONS

The effects of the amplitude g of the high frequency periodic force and the delay-time feedback parameters γ and α on vibrational resonance are explained through a theoretical approach. The theoretical treatment allows us to

predict the values of the control parameters at which resonance occurs, the number of resonances, the parametric choices for which resonance cannot occur, the maximum value of the response amplitude Q, and explains the mechanism of resonance. The theoretical predictions of Q, g_{VR}, and α_{VR} are in very good agreement with the computer simulations. The presence of time-delayed feedback in systems (1) and (2) is found to enrich the vibrational resonance phenomenon. Particularly, the time-delayed parameter α gives rise to a periodic or quasiperiodic pattern of vibrational resonance profile. This feature of vibrational resonance allows us to select different values (small or large) for the delay-time α to enhance the quality of the weak signal and it can be highly useful in optimizing the operation of multistable systems for the detection and regeneration of signals in a variety of experimental systems. The theory accounts for the periodic and quasiperiodic variation of the response amplitude Q. In the overdamped single-well system, resonances cannot occur when g is varied. However, the inclusion of an appropriate time-delayed feedback is found to induce a resonance.

We found the following common results in the four systems that we have analyzed when the time-delayed parameter α is varied: (a)There is no parametric restriction for resonance to occur; (b)The resonance profile is periodic (quasiperiodic) for a rational (irrational) ratio of Ω/ω; (c)The number of resonances in the interval $0 < \alpha < 2\pi/\omega$ is a complicated function of the parameters of the systems; (d)Resonance is due to the local minimization of the quantity S; and (e)Obtaining analytical expressions for α_{VR} and $Q_{\text{max}}(\alpha_{\text{VR}})$ are very difficult.

When the control parameter g is varied, the key results are the following:

(a) Underdamped double-well system (1) ($\omega_0^2 < 0$, $\beta > 0$).

(1) At least one resonance and at most two resonances are possible. The number of resonances is independent of the parameters ω_0^2 and β.

(2) For $|\gamma| < |\gamma_c| = \omega^2/(1 - \cos \omega\alpha)$ two resonances occur at the values of g given by Eqs. (12) due to the matching of ω_r^2 with $\omega^2 - \gamma \cos \omega\alpha$. $Q_{\text{max}} = 1/|-d\omega + \gamma \sin \omega\alpha|$ and is independent of the parameters ω_0^2 and β.

(3) For $|\gamma| > |\gamma_c|$ only one resonance is possible and it always occurs at $g = g_c$ given by Eq. (11) due to the local minimization of ω_r^2 and $Q_{\text{max}} = 1/\sqrt{S}$, where S is given by Eq. (9).

(b) Underdamped single-well system (1) ($\omega_0^2 > 0$, $\beta > 0$). Only one resonance is possible and it occurs at the value of g given by Eq. (16a) provided $\omega^2 - \gamma \cos \omega\alpha > \omega_0^2$. The resonance is due to the matching of ω_r^2 with $\omega^2 - \gamma \cos \omega\alpha$ and $Q_{\text{max}} = 1/|-d\omega + \gamma \sin \omega\alpha|$.

(c) Overdamped double-well system (2) ($\omega_0^2 < 0$, $\beta > 0$). One resonance is always possible and it occurs at $g = g_c$ [given by Eq. (11)], where the effective potential of the slow variable X changes from the double-well to the single-well form. There is no restriction on the parameters ω_0^2 and β. For $\alpha = 2n\pi/\omega$, $n = 0, 1, \ldots$, the resonance is due to the matching of ω_r^2 with $|\gamma| \cos \omega\alpha$ and $Q_{\text{max}} = 1/\omega$. For $\alpha \neq 2n\pi/\omega$, $n = 0, 1, \ldots$, the resonance is due to the local minimization of ω_r^2 and

$$Q_{\text{max}} = \frac{1}{\sqrt{2\gamma^2(1 - \cos \omega\alpha) + \omega^2 - 2\omega\gamma \sin \omega\alpha}} . \quad (24)$$

(d) Overdamped single-well system (2) ($\omega_0^2 > 0$, $\beta > 0$). Only one resonance is possible with g_{VR} given by Eq. (23a) for the parametric restrictions given by Eqs. (23b) and (23c). The resonance is due to the matching of ω_r^2 with $-\gamma \cos \omega\alpha$ and $Q_{\text{max}} = 1/|-\omega + \gamma \sin \omega\alpha|$.

We have investigated here the effect of time delay on VR in systems (1) and (2) with the double-well and single-well cases of the potential of the systems. For $\omega_0^2 > 0$ and $\beta < 0$ the potential of the Duffing oscillator becomes the single well with double hump shown in Fig. 1. We have also studied VR with this potential. Unlike the other two potential types, both systems (1) and (2) with double-hump potential will exhibit bounded motion for $g < g_c = \sqrt{2\mu^2\omega_0^2/(3|\beta|)}$. For $g > g_c$ the effective potential of the slow variable X becomes of an inverted single-well form. In the underdamped double-hump system g_{VR} is given by Eq. (23a) provided $0 < \omega^2 - \gamma \cos \omega\alpha < \omega_0^2$ [compare this condition with Eq. (16b) corresponding to the single-well case]. For the overdamped double-hump system g_{VR} is given by Eq. (23a) provided α lies in the interval given by Eq. (23b) and further, $\gamma < \gamma_c = \omega_0^2/|\cos \omega\alpha|$ [compare this condition with Eq. (23c) to be satisfied for the single-well system].

We believe that the above theoretical and numerical observations will stimulate the experimental study of VR in nonlinear oscillators and electronic circuits with time-delayed feedback. The theoretical approach employed in the present work can also be used to analyze the phenomenon of VR in systems with time-delayed coupling where the interaction between the systems is time delayed.

ACKNOWLEDGMENTS

---

[1] L. Gammaitoni, P. Hanggi, P. Jung, and F. Marchesoni, Rev. Mod. Phys. **70**, 223 (1998).

[2] P. S. Landa and P. V. E. McClintock, J. Phys. A **33**, L433 (2000).

[3] S. Zambrano, J. M. Casado, and M. A. F. Sanjuan, Phys. Lett. A **366**, 428 (2007).

[4] V. N. Chizhevsky and G. Giacomelli, Phys. Rev. E **77**, 051126 (2008).

[5] I. I. Blekhman and P. S. Landa, Int. J. Non-Linear Mech. **39**, 421 (2004).

[6] V. N. Chizhevsky, Int. J. Bifurcation Chaos Appl. Sci. Eng. **18**, 1767 (2008).

[7] S. Jeyakumari, V. Chinnathambi, S. Rajasekar, and M. A. F. Sanjuan, Chaos **19**, 043128 (2009).

[8] S. Jeyakumari, V. Chinnathambi, S. Rajasekar, and M. A. F. Sanjuan, Int. J. Bifurcation Chaos Appl. Sci. Eng. **21**, 275 (2011).

[9] S. Jeyakumari, V. Chinnathambi, S. Rajasekar, and M. A. F. Sanjuan, Phys. Rev. E **80**, 046608 (2009).

[10] V. N. Chizhevsky, E. Smeu, and G. Giacomelli, Phys. Rev. Lett. **91**, 220602 (2003).

[11] V. N. Chizhevsky and G. Giacomelli, Phys. Rev. A **71**, 011801(R) (2005).

[12] V. N. Chizhevsky and G. Giacomelli, Phys. Rev. E **73**, 022103 (2006).

[13] J. P. Baltanas, L. Lopez, I. I. Blechman, P. S. Landa, A. Zaikin, J. Kurths, and M. A. F. Sanjuan, Phys. Rev. E **67**, 066119 (2003).

[14] J. Casado Pascual and J. P. Baltanas, Phys. Rev. E **69**, 046108 (2004).

[15] E. Ullner, A. Zaikin, J. Garcia-Ojalvo, R. Bascones, and J. Kurths, Phys. Lett. A **312**, 348 (2003).

[16] B. Deng, J. Wang, and X. Wei, Chaos **19**, 013117 (2009).

[17] C. Stan, C. P. Cristescu, D. Alexandroaei, and M. Agop, Chaos, Solitons Fractals **41**, 727 (2009).

[18] B. Deng, J. Wang, X. Wei, K. M. Tsang, and W. L. Chan, Chaos **20**, 013113 (2010).

[19] J. H. Yang and X. B. Liu, J. Phys. A: Math. Theor. **43**, 122001 (2010).

[20] J. H. Yang and X. B. Liu, Chaos **20**, 033124 (2010).

[21] J. Chiasson and J. J. Loiseau, *Applications of Time-Delay Systems* (Springer, Berlin, 2007).

[22] *Topics in Time-Delay Systems: Analysis, Algorithms, and Control*, edited by J. J. Loiseau, W. Michiels, S. I. Niculescu, and R. Sipahi (Springer, Berlin, 2009).

[23] F. M Atay, *Complex Time-Delay Systems: Theory and Applications* (Springer, Berlin, 2010).

[24] C. U. Choe, T. Dahms, P. Hovel, and E. Scholl, Phys. Rev. E **81**, 025205(R) (2010).

[25] I. Fischer, R. Vicente, J. M. Buldu, M. Peil, C. R. Mirasso, M. C. Torrent, and J. Garcia-Ojalvo, Phys. Rev. Lett. **97**, 123902 (2006).

[26] R. Vincente, L. L. Gollo, C. R. Mirasso, I. Fischer, and G. Pipa, Proc. Natl. Acad. Sci. USA **105**, 17157 (2008).

[27] V. Flunkert, O. D'Huys, J. Danckaert, I. Fischer, and E. Scholl, Phys. Rev. E **79**, 065201(R) (2009).

[28] D. V. Ramana Reddy, A. Sen, and G. L. Johnston, Phys. Rev. Lett. **85**, 3381 (2000).

[29] M. Gassel, E. Glatt and F. Kaiser, Fluct. Noise Lett. **7**, L225 (2007).

[30] M. Bonnin, F. Corinto, and M. Gilli, Int. J. Bifurcation Chaos Appl. Sci. Eng. **17**, 4033 (2007).

[31] M. A. Dahlem, Philos. Trans. R. Soc. London, Ser. A **367**, 1079 (2009).

[32] K. Pyragas, Phys. Lett. A **170**, 421 (1992).

[33] A. Prasad, J. Kurths, S. K. Dana, and R. Ramaswamy, Phys. Rev. E **74**, 035204(R) (2006).

[34] D. V. Ramana Reddy, A. Sen, and G. L. Johnston, Phys. Rev. Lett. **80**, 5109 (1998).

[35] J. T. Sun, Y. Zhang, and Y. H. Wang, Chin. Phys. Lett. **25**, 2389 (2008).

[36] D. V. Senthilkumar and M. Lakshmanan, Int. J. Bifurcation Chaos Appl. Sci. Eng. **15**, 2895 (2005).

[37] X. Gu, S. Zhu, and D. Wu, Eur. Phys. J. D **42**, 461 (2007).

[38] Y. Jin and H. Hu, Physica A **382**, 423 (2007).

[39] D. Wu and S. Q. Zhu, Phys. Lett. A **363**, 202 (2007).

[40] B. Kelleher, C. Bonatto, P. Skoda, S. P. Hegarty, and G. Huyet, Phys. Rev. E **81**, 036204 (2010).

[41] F. Castro, A. D. Sanchez, and H. S. Wio, Phys. Rev. Lett. **75**, 1691 (1995).

[42] Z. L. Jia, Int. J. Theor. Phys. **48**, 226 (2009).

[43] G. Orosz, J. Moehlis, and F. Bullo, Phys. Rev. E **81**, 025204(R) (2010).